



Article

Integration of Geophysical Survey Data for the Identification of New Archaeological Remains in the Subsoil of the Akrai Greek Site (Sicily, Italy)

Sabrina Grassi ^{1,*}, Gabriele Morreale ¹, Rosa Lanteri ², Angelo Gilotti ³, Federico Latino ¹, Saro Di Raimondo ⁴ and Sebastiano Imposa ¹

¹ Department of Biological, Geological and Environmental Sciences, University of Catania, Corso Italia 57, 95129 Catania, Italy

² Archaeological and Landscape Park of Syracuse, Eloro, Villa del Tellaro and Akrai, Viale Teocrito 66, 96100 Syracuse, Italy

³ Greensol S.R.L., Viale Scala Graca 406/B, 96100 Syracuse, Italy

⁴ Independent Researcher, 97100 Ragusa, Italy

* Correspondence: sgrassi@unict.it

Abstract: For more than a decade now, geophysical prospecting has been considered an integral part of archaeological research; the ability to quickly investigate large areas and locate objects buried in the ground without directly interacting with it is a key feature that makes such surveys essential for identifying and locating, with good accuracy, buried archaeological remains. In this study, two extensive magnetic and electromagnetic surveys were carried out in two different areas of the Akrai archaeological site, where given the distribution of archaeological remains already found at the site, it was likely that additional buried remains were present. The surveys were performed using a proton precession magnetometer and a multifrequency electromagnetic device with a frequency range of 2.5–250 kHz. By processing the data, the vertical magnetic gradient and electrical conductivity maps were obtained. Furthermore, 3D models of electrical conductivity distribution were reconstructed. On comparing the results, it was notable that many anomalies characterized by low vertical gradient values were identified within areas characterized by low electrical conductivity values. These anomalies detected by both surveys can be associated with good probability with buried archaeological remains made up of limestones. In fact, they exhibit shapes and sizes comparable to those of the wall remains already found at the site.

Keywords: Akrai archeological site; geophysical surveys; magnetic method; electromagnetic method; archaeogeophysics



Citation: Grassi, S.; Morreale, G.; Lanteri, R.; Gilotti, A.; Latino, F.; Di Raimondo, S.; Imposa, S. Integration of Geophysical Survey Data for the Identification of New Archaeological Remains in the Subsoil of the Akrai Greek Site (Sicily, Italy). *Heritage* **2023**, *6*, 979–992. <https://doi.org/10.3390/heritage6020055>

Academic Editors: Patrizia Capizzi and Raffaele Martorana

Received: 23 December 2022

Revised: 16 January 2023

Accepted: 22 January 2023

Published: 24 January 2023



Copyright: © 2023 by the authors. Licensee MDPI, Basel, Switzerland. This article is an open access article distributed under the terms and conditions of the Creative Commons Attribution (CC BY) license (<https://creativecommons.org/licenses/by/4.0/>).

1. Introduction

Geophysical prospecting is considered a very important tool in support the archaeological research given its noninvasiveness, speed of execution, and the continuous technological progress of instrumentation. Different geophysical survey methodologies adopted in archaeology over the past 60 years, such as the electrical resistivity technique [1,2], ground-penetrating radar (GPR) [3–5], electromagnetic method [6,7], and magnetism [8], can be used to correctly map the position and geometry of buried remains, enabling accurate archaeological excavations [3,9–17]. Usually, the materials of buried archaeological finds generate contrasts with the surrounding soil due to differences in physical and mechanical properties. The anomalies generated by these contrasts enable locating archaeological remains that have not yet been unearthed [18].

Among the techniques just mentioned, the electromagnetic method has a wide range of applications; it succeeds in providing detailed information on the spatial variability of soil properties such as water content [19], degree of lithotype compaction [20], and lithological

differences [21], and given its speed of execution and noninvasiveness, it represents one of the most advantageous methods. Another very efficient method in archaeological research is the magnetic method, which by exploiting the differences between the magnetic properties of buried targets and those of the surrounding lithotypes is able to provide excellent mapping of archaeological remains underground [22,23].

These surveys represent fundamental tools for detecting and characterizing archaeological structures and for preliminary mapping of areas to be excavated.

The investigated area, known as the “Akrai Archeological site”, is an ancient Greek city founded in 663–664 B.C. The site lies on a plateau to the west of the Palazzolo Acreide municipality, located in the southeast of Sicily (Italy), on an elevation of about 670 m above sea level (Figure 1a,b). From a geological point of view, the investigated area is part of the Hyblean Plateau, which represents a portion of the uplifted Sector of the Pelagian Block and consists of Lower Triassic–Jurassic platform limestones with intercalations of basic volcanites (Figure 1c) [24,25].

Some archaeological excavations, performed in the Akrai archeological site area, have unearthed numerous archaeological structures dating to the Hellenistic and Roman imperial eras [26], but the true extent of the ancient Greek city has not yet been identified.

This study aims to detect areas characterized by the presence of buried structures by correlating archaeological knowledge of the site and the results obtained by magnetic and electromagnetic geophysical surveys.

These methods prove of significant importance in the archaeological field because they enable investigating large areas fairly quickly and without interacting with the subsoil in any way [18,27,28]. The two methods used are based on different physical principles, consequently, the result of the individual investigation is influenced by the distribution of a specific physical property related to the materials present in the subsurface. These methods, considered individually, tend to highlight anomalies related to the presence of objects in the subsurface that are not always of archaeological interest. It was therefore necessary to carry out an integration of the results to exclude anomalies generated by the presence of targets of different origins and to constrain anomalies attributable to archaeological remains.

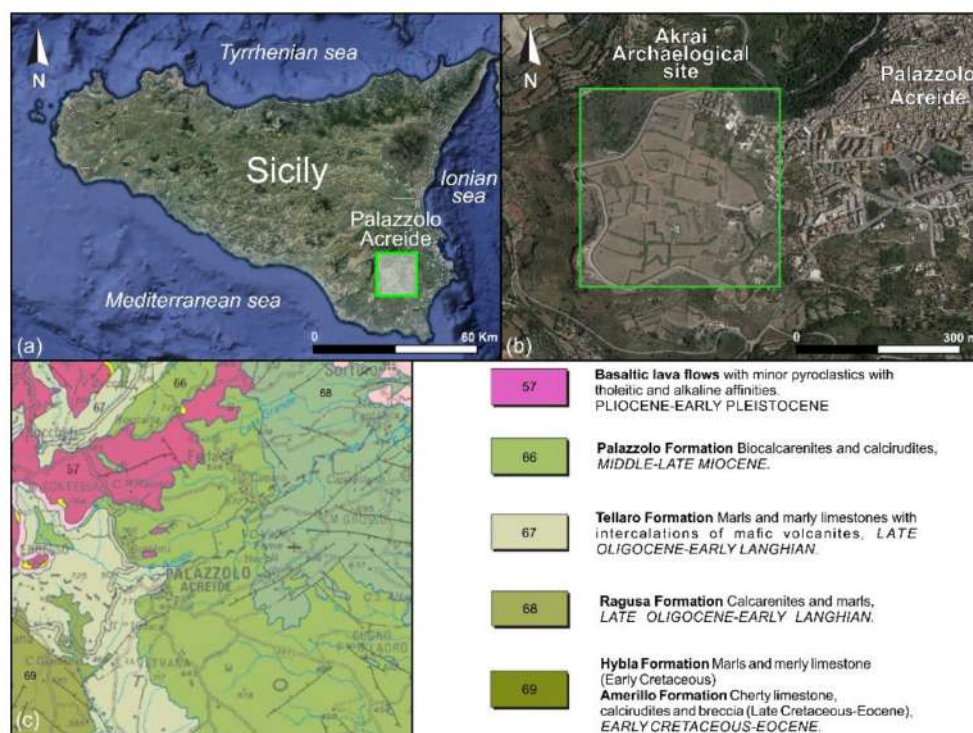


Figure 1. (a) Location of Palazzolo Acreide municipality; (b) position of Akrai archaeological site; (c) geological map of the area (scale 1:250,000) (modified from [25]).

2. The Archaeological Site

Syracuse, the Greek city founded by the Corinthians in the southeastern coast of Sicily (Italy) in 734 B.C., as the Greek historian Thucydides relates, 70 years later founded the sub colony Akrai (664–663 B.C.), about 35 km west inland. Akrai, connected to Syracuse by the so-called *via acense*, was founded for strategic purpose. In fact, it stands on a hill (about 670 m above sea level) from which it is possible to oversee the whole surrounding area and to check the road connecting with the interior and the south coast of the island (via *selinuntina*). The city reached its maximum expansion during the reign of Hiero II, a period during which the most important public buildings were built (Figure 2a). After the Roman conquest of Sicily, Akrai became a *civitas stipendiaria*, required to pay a fixed tax to Rome. The archaeological evidence indicates a continuity of life of the city through the Byzantine period and until later times to the Arab conquest. The highlighting of the city began in the early XIX century, when the Baron Gabriele Judica discovered some important public buildings (i.e., the theater and bouleuterion), but archaeological investigations conducted using scientific methods were carried out for the first time by Luigi Bernabò Brea in the 1950s of the XX century [26]. Bernabò Brea investigated, among the other monuments, the Aphrodite's temple on the acropolis of the city. Afterwards, the excavation in the 1960s and 1970s of the XX century carried out by the Superintendence of Cultural Heritage of Syracuse were focused on the central part of the urban plan and brought the main road to light (*decumanus*). Recently, the Italian–Polish archaeological mission investigated an urban block on the west side of the city [29].

In the eastside of the city's plateau, are the "latomie" (quarries), in use since the foundation of the city for the extraction of limestone blocks (Figure 2b). In the Hellenistic period (between the 3rd and 1st century B.C.), the area became a place of worship for the heroized deceased, as evidenced by the dozens of quadrangular niches dug into the walls of the quarries, inside which were small votive reliefs (pinakes) of stone, terracotta or wood. During the Roman period, probably from the 3rd century A.D. onwards, the mining activity ceased, and the quarries were exclusively used as a necropolis area with burial chambers and hypogea. Some of them, starting in the Byzantine period, were transformed into dwellings for the poorest people [30]. To the west of the quarries is the Greek theatre (Figure 2c,d), built during the reign of Hiero II (3rd century B.C.), but modified in the Roman and Byzantine periods. The current state is due to the restoration carried out by Barone Judica in the 19th century. The natural slope of the hill was exploited for the construction of the *cavea*, divided into nine vertical sectors by eight stairways and capable of holding around 600 spectators. The theatre faces north, and it has a perfectly semicircular shape, a feature that distinguished it from the other Greek theaters in Sicily. Near the theatre is the bouleuterion (Figure 2e), the meeting place of the city's senate (*boulè*). It consists of a quadrangular building, originally covered, inside which there is a semicircular *cavea* of six steps divided into three wedges by two small stairs. Like the theatre, it was built in the Hellenistic period. The entire urban area is crossed from east to west by the *decumanus* (main road), which was brought to light for a length of about 250 m. The average width is 4 m and it was paved with polygonal basaltic stones. It also connects the two main gates opened in the walls of Akrai: the "Selinuntina" gate on the west side and the Syracusan gate on the east side. This main road dates back to the Roman period, but probably remakes the older Greek road (*plateia*). The *decumanus* is crossed by smaller roads (*cardines*), about 3 m large, at a regular distance of 25 m corresponding to the width of each urban block. These smaller roads are not exactly orthogonal to the *decumanus*, but slightly inclined NW–SE, probably to contrast the strong and cold north wind. South of the main road, there is a wide central area identified as the city's public square (*agorà*). Some remains of various buildings, mainly serving public functions, were found here. The most recent date back to the Byzantine period. In particular, a large circular building, of which only the basement remains, has been interpreted as a Roman bath, transformed into a baptistery in the Byzantine period. In the same period, a Christian catacomb was excavated into the face of a small quarry located on the back of the circular building (Figure 2f,g). The

remains of the temple dedicated to Aphrodite were identified on the top of the acropolis, in the area overlooking to the theater from the south side (Figure 2h). Only a few regular stone blocks and some traces of the flat ground where these blocks were laid can be seen today. Over the centuries, the building stones were removed and used to build new homes when the city moved to the east, where today Palazzolo Acreide stands. The temple of Aphrodite was a Doric temple (18.30×39.50 m) with 6 columns on the short side and 13 on the long side. On the front there was a double order of six columns. Its construction dates back to the second half of the 6th century B.C. In the area between the temple of Aphrodite and the theater, a Hellenistic sanctuary (probably a Thesmophorion) was found (Figure 2h), which was accessed through a colonnade (stoà) on the East. The sanctuary consists of about 25 rooms: those in the central area were perhaps intended for the purification rites, the remaining rooms for animal sacrifices, sacrificial meat cooking and votive terracotta storage. In this sanctuary, dedicated to Demetra and Kore, the rites of the Thesmophorie were performed by women, eugeneis (well-born), gametai (well-married), and astai (full rights citizens) [31]. In recent years, researchers have mainly focused on understanding ancient urban planning, but most of the city has not yet been excavated (Figure 2g).

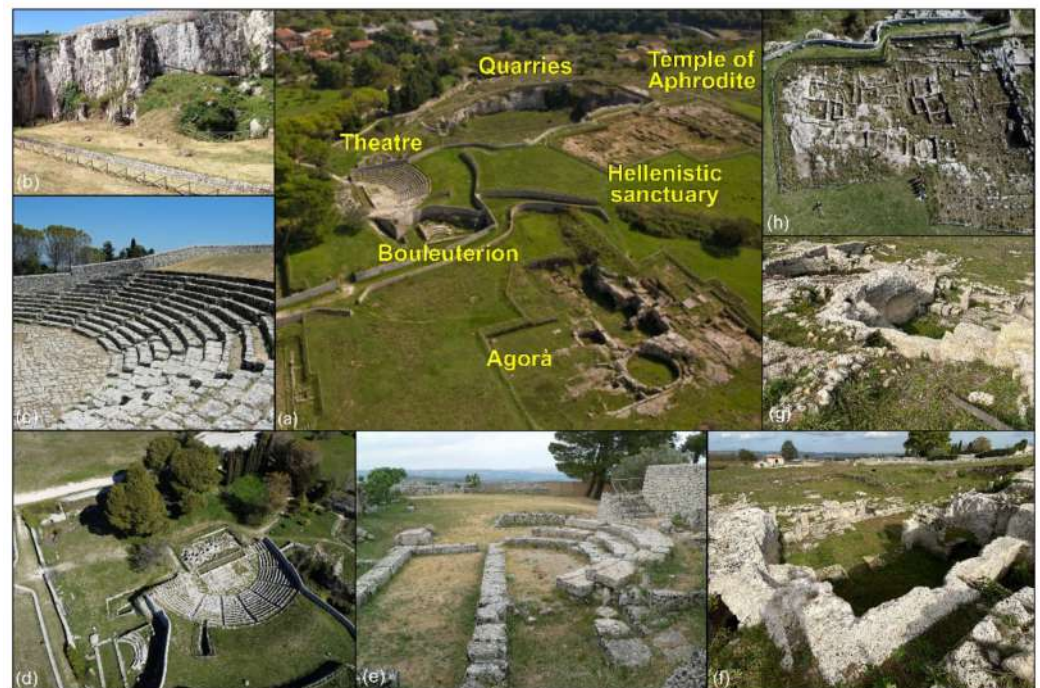


Figure 2. (a) Location of discovered archaeological remains; (b) stone quarries; (c,d) theatre viewed from different angles; (e) photo of bouleuterion; (f,g) archaeological remains already unearthed near the investigated site; (h) Hellenistic sanctuary and temple of Aphrodite viewed from above.

3. Geophysical Methods

3.1. Magnetic Survey

The magnetic method represents one of the most widely used and efficient applied geophysics survey techniques for characterizing archaeological sites since the differences in magnetic properties between buried remains and surrounding lithotypes can generate magnetic anomalies [32,33].

The presence of archaeological remains buried in the subsoil is capable of producing a wide range of magnetic gradient values [34,35]. The contrast in magnetic susceptibility between different materials allows for the detection of presence in the subsurface of trenches and cavities filled with surface material. Filled subsurface sectors generate positive anomalies while materials with poor magnetic properties such as limestones can generate negative magnetic anomalies in many cases [35,36].

The presence of archaeological remains associated with floors and wall structures usually generates anomalies between 1–20 nT. Instead, the presence of ferromagnetic targets such as weapons and items such as pottery and ovens tend to generate much more significant magnetic anomalies, in the range of 10–2000 nT [34].

The gradiometric method is one of the most widely used configurations for the application of the magnetic method in archaeology because it makes the measuring data independent of anthropic noise and temporal magnetic field fluctuations [18]. Compared with other techniques such as measuring total magnetic intensity, the gradiometric method is characterized by a higher horizontal resolution of anomalies, does not require the application of a correction for diurnal variations in the magnetic field, and allows an “anomaly” value to be obtained directly.

This technique consists of measuring the vertical gradient of the Earth’s magnetic field using a system consisting of two coils. Considering that the decay of the vertical magnetic gradient occurs with the fourth power of the distance from the source-producing the anomaly, it allows us to enhance surface anomalies, which are generated by archaeological targets, over deeper anomalies [18].

Given the position of the archaeological remains currently found at the site (Figure 2a), it was decided to focus the magnetic survey in two areas, the first located to the southeast of the “Agorà” and the second to the west of the “Temple of Aphrodite” (Figure 3a).

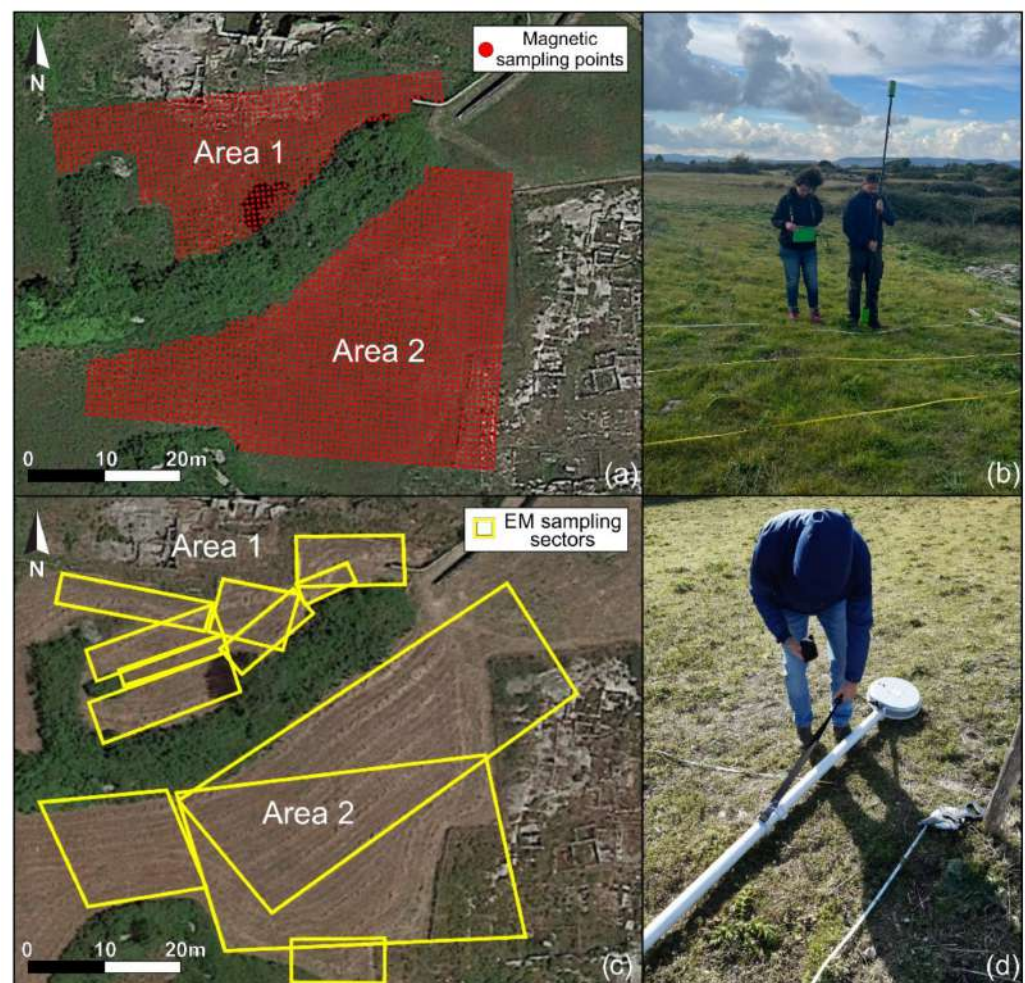


Figure 3. (a) Acquisition grid of magnetic data points; (b) photo of magnetic survey; (c) location of electromagnetic survey sectors and (d) photo of electromagnetic survey.

The magnetic data acquisition was performed using an acquisition scheme for each area, consisting of parallel profiles spaced 1 m apart with a distance between measuring

points along the lines of 1 m (Figure 3a). This sampling interval was chosen considering the dimensions of archaeological remains already discovered in the surroundings of the investigated area. The acquisition schemes were specially designed to include portions of archaeological remains already unearthed in previous excavation campaigns, to calibrate the instrument and have a comparison with the gradient values generated by buried targets.

In the first area, the survey included the acquisition of 1608 magnetic data points (Figure 3a), while in the second area 2208 magnetic data points (Figure 3a) were acquired, and each measurement point was georeferenced using a GNSS device.

The magnetic methodology was applied in gradiometric configuration using a PMG2 proton magnetometer and gradiometer, characterized by an absolute accuracy of ± 1 nT. Two measuring sensors (coils), a processing unit, and a post (Figure 3b) comprise the instrument; the coils were spaced 2.30 m apart. This approach allows for obtaining vertical gradient values independent of diurnal variations in the Earth's magnetic field. Magnetic data were acquired in a single direction by orienting the coils north, which avoided the noise associated with bidirectional acquisition.

The magnetic data sets were processed using Magpick software "www.geometrics.com (accessed on 2 September 2022)". Based on the acquisition mode, it was not necessary to apply functions to eliminate stripes and zigzag effects. The data were processed by applying a cubic smoothing spline function and subsequently gridded to each area to obtain maps of the magnetic gradient.

3.2. Electromagnetic Survey

The electromagnetic survey method is another of the most popular techniques used in archaeological research. It is able to identify the contrast of magnetic and electrical properties between buried structures and the surrounding materials [37,38].

This approach is used to measure the electric currents produced in the subsoil by the induction of electromagnetic fields, using transmitting and receiving coils in the frequency domain (FDEM) [36]. It is preferred to the magnetic method in cases where there is a presence in the subsurface of the wall remains composed of lithotypes with high resistivity values surrounded by materials with poor physical–mechanical features.

The transmitting coil produces a primary electromagnetic wave generating the flow of eddy currents in the conductive materials in the subsurface. As a result, a secondary electromagnetic field is produced, which is recorded by the receiver and analyzes in-phase (real) and quadrature (imaginary) components.

The in-phase component proves to be sensitive to magnetic objects and is expressed in ppm (parts per million), while the quadrature component is sensitive to electrically conductive objects, expressed in mS/m (millisiemens per meter) [39].

Multifrequency instruments provide a theoretical depth of investigation using very wide frequency ranges and can produce a very detailed subsoil scan. Indeed, high frequencies allow good quality data to be obtained at shallow depths, while lower frequencies enable obtaining data at higher depths [40].

The electromagnetic data acquisition was carried out by dividing the same areas into small sectors that partially overlap each other. For each sector, the data were acquired along linear profiles with a distance between measuring points of 1 m (Figure 3c).

The area located near the "Agorà" was divided into 8 sectors, while the second area was divided into 4 sectors. For electromagnetic data acquisition, an AEMP14 multifrequency electromagnetic device was used. This device consists of three coils, one a transmitter and the others receivers, and is equipped with an integrated GPS system; the distance between the transmitting coil and the first receiving coil is 1.5 m, while the distance to the second receiving coil is 2.5 m (Figure 3d). It is capable of working on 14 defined frequencies in a range of 2.5–250 kHz; each antenna with increasing frequency corresponds to a surveyed depth of about 0.70 m.

Unfortunately, in Area 1 (Figure 3c), due to integrated GPS system signal problems, it was not possible to acquire the coordinates of each measurement point. Only the coordi-

nates of the vertices of the sectors into which the area was divided were recorded using a GNSS device, the other measuring points were located considering the used sampling step. Instead, coordinates were acquired for all measurement points in Area 2.

The acquired data were processed by analyzing the quadrature component for each sector, obtaining electrical conductivity maps. The maps refer to electrical conductivity values measured by the highest frequency antenna (250 kHz). Moreover, the individual maps were overlapped, according to the acquisition scheme, to obtain the trend of the conductivity values in the investigated areas (Figure 3c).

A 3D subsoil model was obtained for each sector of Area 1, while for Area 2, having georeferenced all acquisition points, it was possible to obtain a 3D subsurface model for the whole area. For the construction of the 3D models, the electrical conductivity values measured from antennas 11, 12, 13, and 14, corresponding to frequencies 40–62.5–111.11–250 kHz, were plotted using Voxler 4 software (www.goldensoftware.com).

4. Results and Discussion

The vertical magnetic gradient data were interpolated and plotted in the range between -20 and 20 nT/m, to obtain the distribution of magnetic gradient values in both investigated areas (Figure 4). The maps show the presence of numerous areas characterized by negative vertical magnetic gradient anomalies; the anomalies with larger negative values were highlighted.

The already-discovered archaeological ruins located in the surroundings of the investigated area are characterized by the presence of structures built with limestone blocks. As observed by other authors (e.g., [35,36]), the presence of buried limestone walls can produce negative magnetic anomalies. In the northern portion of Area 1, two linear anomalies oriented around WNW–ESE with negative values can be observed (dashed red lines in Figure 4); the westernmost anomaly extends for about 7 m, while the second one extends for a length of about 10 m. These anomalies correspond to limestone walls that had already been uncovered in previous archaeological digs and were used as guidelines for the tracing of the other anomalies.

In the central portion of Area 1, the presence of linear negative magnetic gradient anomalies is observed, some of them oriented around N–S and others E–W (green dashed lines in Figure 4). The N–S-oriented anomalies are about 10 m long while the approximately E–W-oriented anomalies extend for a length of about 8 m.

In the northwestern portion of the area, we observe the presence of many negative anomalies, some linear with N–S and E–W orientation, extending in both directions for about 3 m in length (green dashed lines in Figure 4), and others more extensive (blue dashed squares in Figure 4), with lower values compared to the anomalies discussed so far.

The shape and direction of the identified anomalies turns out to be fully compatible with the structures visible to the north of the investigated area belonging to the “Agorà”.

In Area 2, similarly to Area 1, the data acquired at a limestone wall that has already been unearthed shows a negative linear anomaly of the vertical magnetic gradient in the southeastern portion of the area (dashed red line in Figure 4). In general, the area shows a wide distribution of negative linear anomalies similar to the previous one, characterized in most cases by an N–S and E–W orientation, forming regular geometries (dashed green lines in Figure 4).

In the western portion of Area 2, the map shows the presence of several anomalies characterized by negative gradient values. These linear anomalies, which appear to be interconnected with each other, show an extension in length in the range of 3–10 m. In the central portion of the area, the presence of linear anomalies with negative magnetic gradient values is clear; these anomalies appear to connect with each other and enclose an anomaly characterized by positive magnetic gradient values. The negative anomalies just described show an extension in both directions of about 7 m (Figure 4).

Other anomalies with magnetic features similar to those just described can be seen in the southeastern portion of the area. These anomalies extend in length in both directions

in a range of 6–10 m and, like the previous ones, appear to be interconnected, forming regular geometries.

Also in Area 2, the identified anomalies are comparable in size and shape with the archaeological remains already unearthed east of the investigated area, identified as belonging to the “Hellenistic sanctuary”.

The anomalies characterized by low vertical magnetic gradient values, highlighted by the maps shown in Figure 4, many of which appear to be linked by assuming linear geometries, can be ascribed to the possible presence of ancient buried wall structures. In both areas, the anomalies just described seem to enclose anomalies with positive magnetic gradient values, indicative of the presence of backfill material with ferromagnetic features. Since these positive anomalies are isolated and often bordered by negative gradient anomalies; this allows us to suppose the possible presence of filled ancient rooms with material characterized partially by ceramic objects [18].

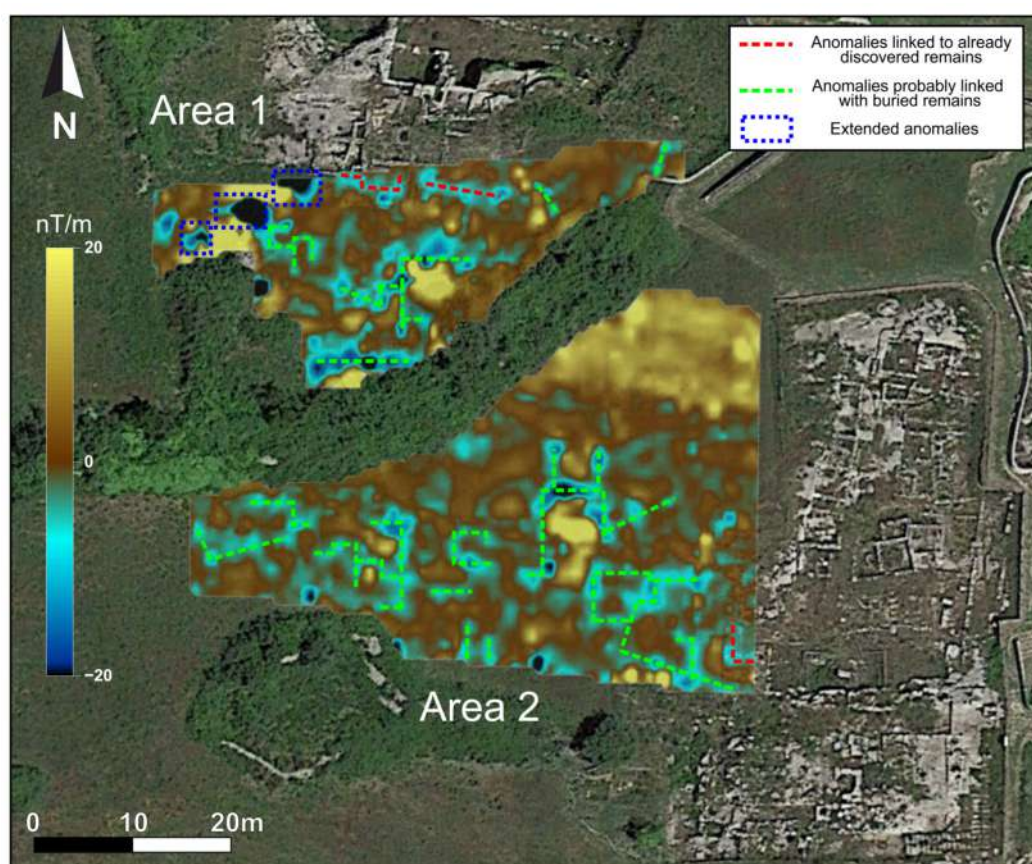


Figure 4. Vertical gradient maps of both areas.

The electrical conductivity data were plotted for each sector and later overlapped to obtain the distribution of electrical conductivity values in the investigated areas (Figure 5).

The electrical conductivity map for Area 1 shows the presence of several anomalies characterized by low conductivity values. The northeastern portion of the area shows the presence of two low conductivity zones separated by an anomaly characterized by higher conductivity values. The eastmost anomaly extends about 8 m in a N–S direction and 12 m in an E–W direction; it in part appears to assume a linear geometry oriented about NW–SE. The second anomaly also appears to be oriented in the NW–SE direction with an extension in width of about 9 m (Figure 5).

Another anomaly with low electrical conductivity values is observed in the western portion of the investigated area. The anomaly extends in the NNE–SSW direction for about 12 m in length and in the E–W direction for about 8 m (Figure 5).

A high-conductivity anomaly characterizes the south-central portion of Area 1, separating the previously identified low-conductivity anomalies. The highest electrical conductivity values are observed in the westmost part of the area.

The map obtained for Area 2 highlights the presence of several electrical conductivity anomalies. In the eastern portion of the area, the presence of a marked anomaly characterized by low electrical conductivity values is observed. (Figure 5). This anomaly is bordered to the north by an anomaly with high conductivity values extending in a NE–SW direction for about 18 m.

The central portion of the area is characterized by high electrical conductivity values, extending with a NE–SW orientation (Figure 5).

To the west of this area, there is an additional anomaly characterized by low conductivity values, which is less clear than the first anomaly described. This anomaly extends about 8 m in the N–S direction and about 13 m in the E–W direction (Figure 5).

Moreover, a slight anomaly characterized by high conductivity values is observed in the extreme western portion of the area.

The electrical conductivity maps highlighted many anomalies characterized by low conductivity values alternating with positive anomalies. In agreement with other authors (e.g., [36]) the low conductivity anomalies can be related to the possible presence of limestone walls buried underground. Areas characterized by higher conductivity values may be associated with the presence of fill soil.

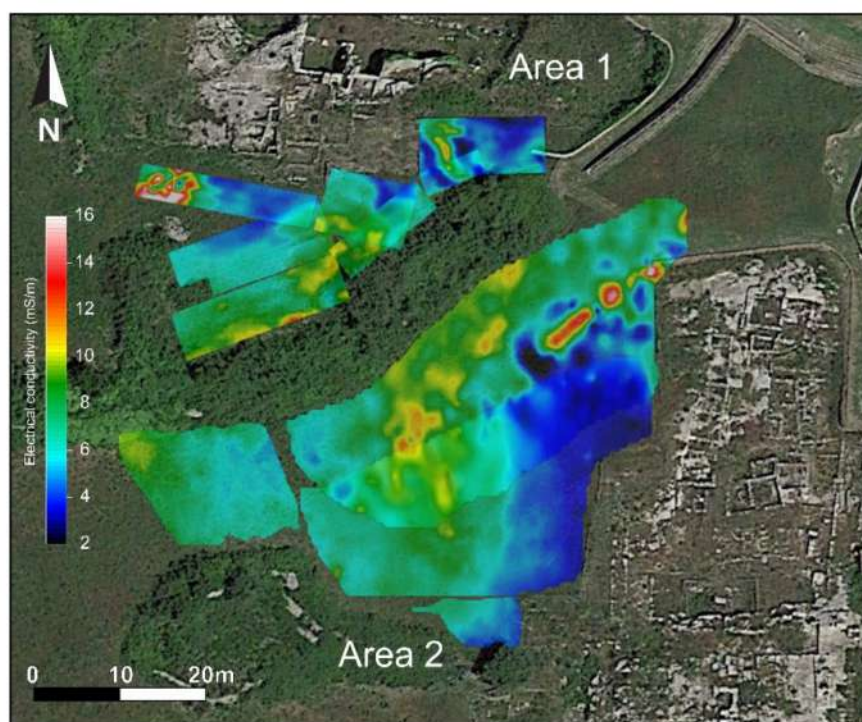


Figure 5. Electrical conductivity maps of the investigated areas.

As mentioned in Section 3.2, for Area 1 it was not possible to acquire the coordinates of all measurement points, so 3D models showing the trend of electrical conductivity values in depth were obtained for each Sector (Figure 6a–h), into which the investigated area was divided. In this way, it was possible to highlight the distribution in the three dimensions of low conductivity areas more clearly, which may be associated with the presence of possible buried archaeological remains consisting of limestone blocks.

The 3D model for Sector a (yellow rectangle in Figure 6) shows the presence of two areas characterized by low electrical conductivity values. The first area is located in the southwestern part of the sector, while the second area extends from N to S along the entire section length assuming a linear geometry toward the south. The model for Sector b

(green rectangle in Figure 6) shows the presence of a significant anomaly characterized by low electrical conductivity values in the approximately NW–SE direction, which seems to represent a continuation of the anomaly visible in Sector a. In Sector c (light purple rectangle in Figure 6), the model shows the presence of only one anomaly characterized by similar electrical conductivity values compared with the anomalies described so far in the other sectors. This isolated anomaly is visible in the northeastern portion of the model. In Sector d (magenta rectangle in Figure 6), a fairly extended area characterized by low electrical conductivity values is observable in the southwestern portion.

The 3D model for Sector e (orange rectangle in Figure 6) highlights the presence of two anomalies with low electrical conductivity values. The first anomaly is located in the northwestern portion of the sector while the second is in the central portion; this anomaly, larger than the previous one, extends in an approximately NW–SE direction.

In Sector f (blue rectangle in Figure 6) a large low electrical conductivity anomaly extends from the center to the eastern end of the model. The model of Sector g (red rectangle in Figure 6) shows the presence of a single anomaly characterized by low electrical conductivity values located in the south-central portion of the area that seems to be a continuation of the anomaly described in the adjacent Sector f. The last model, of Sector h (light blue rectangle in Figure 6), highlights the presence of an anomaly with low electrical conductivity values extending from the west end to the center of the investigated portion, while the remaining part of the model does not show anomalies with properties similar to those already described.

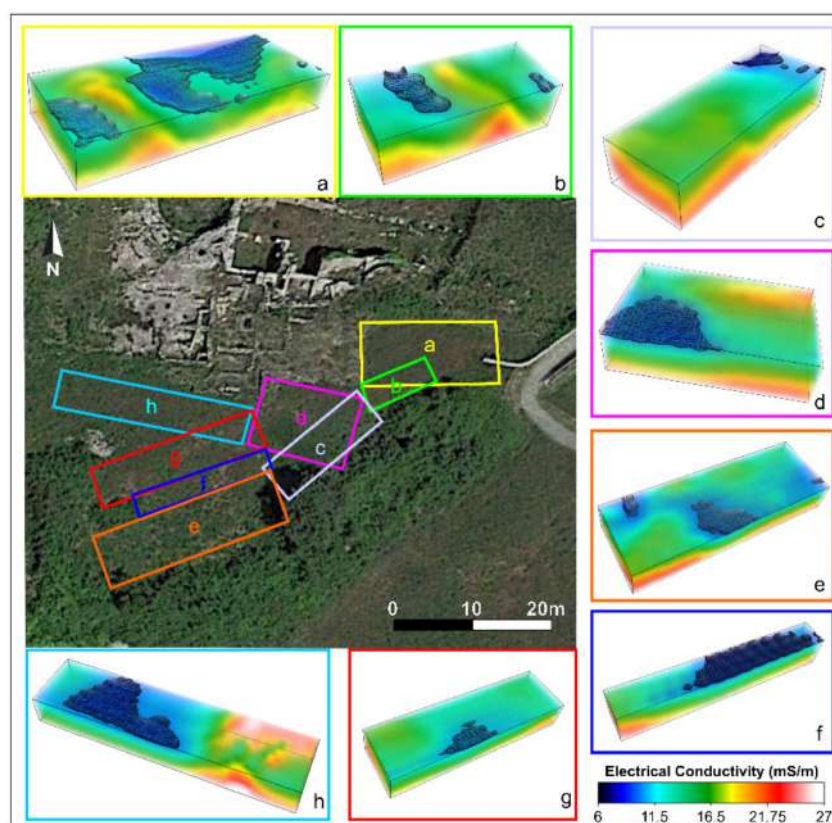


Figure 6. Three-dimensional electrical conductivity models for each sector (a–h) of Area 1.

For Area 2, it was possible to obtain a single 3D subsoil model showing the trend of electrical conductivity values in the area (Figure 7).

The model shows the presence of two large anomalies characterized by low electrical conductivity values, one located in western portion of the investigated area and another to the northeastern portion. (Figure 7).

This anomaly is very extensive below the surface and appears to be oriented in the NE–SW direction. To the south of this area, less aerially extensive electrical conductivity anomalies are visible, which appear to be related to the previous one in depth (Figure 7).

Moreover, by analyzing the model, it is possible to identify the presence of numerous—much smaller in size— anomalies than those described so far, which could be associated with individual limestone blocks scattered throughout the investigated site and resulting from the decay of preexisting structures. Throughout the central area, instead, the model does not highlight the presence of low electrical conductivity anomalies, suggesting the absence of archaeological remains consisting of limestone blocks buried underground.

The results of the magnetic survey suggest the presence of anomalies located at shallow depths. This is confirmed by the electromagnetic data, as the anomalies are highlighted by the data acquired through the higher frequency antennas. Moreover, considering the topographical features of the site in relation to the elevation of the archaeological remains already unearthed around the investigated areas, the anomalies highlighted by the results could be attributable to archaeological targets localized within the first two meters of depth.

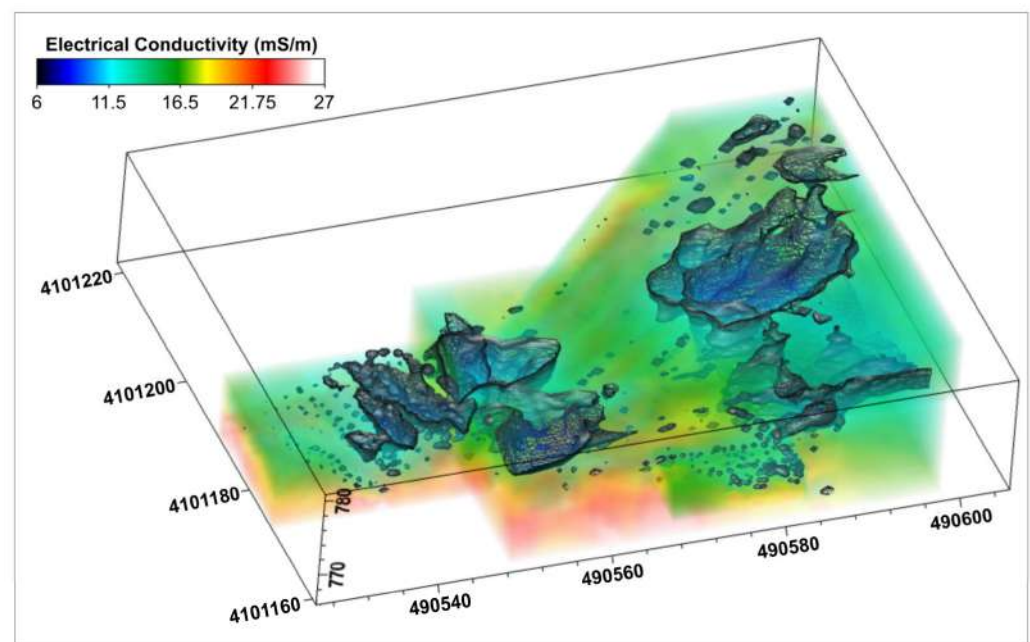


Figure 7. Three-dimensional electrical conductivity model of Area 2.

5. Conclusions

The integration of the results of geophysical surveys carried out at the Akrai archaeological site allowed for identifying many anomalies most likely linked to the presence of buried archaeological remains.

As described in Section 4, gradiometric measurements performed in the studied site, on already-discovered portions of archaeological remains, produced negative magnetic gradient values. These data were used as a guideline for the interpretation of the anomalies that were identified in the investigated areas. The size and linear trend of the identified anomalies indicate with good probability the presence of limestone wall structures in the subsurface. The width of these anomalies, around one meter, is also compatible with the dimensions that characterize the wall remains found around the investigated areas. In addition, the electrical conductivity maps highlighted many anomalies characterized by low conductivity values, which according to the literature data can be associated with the possible presence of limestone targets buried in the investigated site. The surveys revealed an excellent overlap and continuity between anomalies in corresponding and adjacent areas in both investigated areas, as well as a clear spatial continuity with the archaeological remains already unearthed.

Interpretation of the electromagnetic survey results was more complex than of the magnetic survey, because the linear trend of the anomalies found by the gradiometric measurements left a few interpretive doubts. In this case, the extensive anomalies characterized by lower electrical conductivity values could refer to the complex of the walls, pavement, and foundations, consisting of limestone, which causes a lowering in the values found by the survey.

Considering the location of the archaeological remains already identified in previous archaeological digs, located around the investigated area, and the position of the detected anomalies, it is reasonable to assume that the conductivity anomalies visible in Area 1 could represent another part of the complex of structures located north of the studied area.

Similarly, the largest low electrical conductivity anomaly located in the easternmost portion of Area 2, given its shape and position, might represent a possible continuation of the “Hellenistic sanctuary” already brought to light to the east of this anomaly. Another similar anomaly is observed in the western portion of the area, also attributable to the possible presence of buried limestone structures probably linked to the remains visible to the south of the anomaly itself.

By comparing the results of both methodologies used to investigate the site, it can be seen that almost all the negative vertical magnetic gradient anomalies are located within the area characterized by low electrical conductivity values. The matching of the anomalies found allows validating the data obtained and reducing the uncertainty related to the detection of buried structures. In addition, the georeferencing of the data made it possible to locate the anomalies identified with good accuracy.

The results obtained provide important insights that can be used to support the planning of future archaeological digs.

Author Contributions: Conceptualization, S.G., G.M. and S.I.; methodology, S.G., G.M., A.G. and S.I.; validation, S.G., G.M. and S.I.; investigation, S.G., G.M., A.G., F.L., S.D.R. and S.I.; data curation, S.G., G.M. and S.I.; writing—original draft preparation, S.G. and G.M.; writing—review and editing, S.G. and G.M.; visualization, S.G., G.M. and S.I.; supervision, S.G., G.M., R.L. and S.I. All authors have read and agreed to the published version of the manuscript.

Funding: This research received no external funding.

Data Availability Statement: The data presented in this study are available upon request from the corresponding author.

Acknowledgments: The authors wish to thank the Parco Archeologico e Paesaggistico di Siracusa, Eoro, Villa del Tellaro e Akrai for allowing the surveys to be carried out. Thanks to Stephen Conway for reviewing the English text.

Conflicts of Interest: The authors declare no conflict of interest.

References

1. Hesse, A. Count Robert du Mesnil du Buisson (1895–1986), a French precursor in geophysical survey for archaeology. *Archaeol. Prospect.* **2000**, *7*, 43–49. [[CrossRef](#)]
2. Masini, N.; Capozzoli, L.; Chen, P.; Chen, F.; Romano, G.; Lu, P.; Tang, P.; Sileo, M.; Ge, Q.; Lasaponara, R. Towards an operational use of Remote Sensing in Archaeology in Henan (China): Archaeogeophysical investigations, approach and results in Kaifeng. *Remote Sens.* **2017**, *9*, 809. [[CrossRef](#)]
3. Castellaro, S.; Imposa, S.; Barone, F.; Chiavetta, F.; Gresta, S.; Mulargia, F. Georadar and passive seismic survey in the Roman Amphitheatre of Catania (Sicily). *J. Cult. Herit.* **2008**, *9*, 357–366. [[CrossRef](#)]
4. Urban, T.M.; Murray, C.A.; Vella, C.; Lahikainen, A. Ground-penetrating radar survey on the island of Pantelleria (Italy) reveals an ancient architectural complex with likely Punic and Roman components. *J. Appl. Geophys.* **2015**, *123*, 164–169. [[CrossRef](#)]
5. Leucci, G.; Di Giacomo, G.; Ditaranto, I.; Miccoli, I.; Scardozzi, G. Integrated Ground-penetrating Radar and Archaeological Surveys in the Ancient City of Hierapolis of Phrygia (Turkey). *Archaeol. Prospect.* **2013**, *20*, 285–301. [[CrossRef](#)]
6. Simpson, D.; Lehouck, A.; Meirvenne, M.V.; Bourgeois, J.; Thoen, E.; Vervloet, J. Geoarchaeological prospection of a medieval manor in the Dutch Polders using an electromagnetic induction sensor in combination with soil augerings. *Geoarchaeol.–Int. J.* **2008**, *23*, 305–319. [[CrossRef](#)]

7. Tang, P.; Chen, F.; Jiang, A.; Zhou, W.; Wang, H.; Leucci, G.; De Giorgi, L.; Sileo, M.; Luo, R.; Lasaponara, R.; et al. Multi-frequency Electromagnetic Induction Survey for Archaeological Prospection: Approach and Results in Han Hangu Pass and Xishan Yang in China. *Surv. Geophys.* **2018**, *39*, 1285–1302. [CrossRef]
8. Rizzo, E.; Chianese, D.; Lapenna, V. Integration of magnetometric, GPR and geoelectric measurements applied to the archaeological site of Viggiano (Southern Italy, Agri Valley-Basilicata). *Near Surf. Geophys.* **2005**, *3*, 13–19. [CrossRef]
9. Capozzoli, L.; De Martino, G.; Capozzoli, V.; Duploux, A.; Henning, A.; Rizzo, E. The pre-Roman hilltop settlement of Monte Torretta di Pietragalla: Preliminary results of the geophysical survey. *Archaeol. Prospect.* **2020**, *9*, 45–53. [CrossRef]
10. Colombero, C.; Elia, D.; Meirano, V.; Sambuelli, L. Magnetic and radar surveys at Locri Epizephyrii: A comparison between expectations from geophysical prospecting and actual archaeological findings. *J. Cult. Herit.* **2020**, *42*, 147–157. [CrossRef]
11. Grassi, S.; Imposa, S.; Patti, G.; Boso, D.; Lombardo, G.; Panzera, F. Geophysical surveys for the dynamic characterization of a cultural heritage building and its subsoil: The S. Michele Arcangelo Church (Acireale, eastern Sicily). *J. Cul. Herit.* **2019**, *36*, 72–84. [CrossRef]
12. Imposa, S.; Grassi, S.; Patti, G.; Boso, D. New data on buried archaeological ruins in Messina area (Sicily-Italy) from a ground penetrating radar survey. *J. Archaeol. Sci. Rep.* **2018**, *17*, 358–365. [CrossRef]
13. Imposa, S.; Grassi, S.; Di Raimondo, S.; Patti, G.; Lombardo, G.; Panzera, F. Seismic refraction tomography surveys as a method for voids detection: An application to the archaeological park of Cava Ispica, Sicily, Italy. *Int. J. Archit. Herit.* **2018**, *12*, 806–815. [CrossRef]
14. Imposa, S.; Grassi, S.; Barone, I.; Censini, M.; Morreale, G. Combined GPR and seismic refraction tomography to study the subsoil in the Cathedral of S. Giorgio Ragusa-Ibla (Sicily). In Proceedings of the 11th International Workshop on Advanced Ground Penetrating Radar (IWAGPR), Valletta, Malta, 1–4 December 2021; pp. 1–3. [CrossRef]
15. Imposa, S.; Gilotti, A.; Lanteri, R.; Morreale, G.; Grassi, S.; Latino, F.; Romano, F.; Di Raimondo, S. Magnetic and Electromagnetic Surveys at the Akrai Archaeological Site (Sicily-Italy). European Association of Geoscientists & Engineers. Conference Proceedings. In Proceedings of the NSG2022 28th European Meeting of Environmental and Engineering Geophysics, Belgrade, Serbia, 18–22 September 2022; pp. 1–5. [CrossRef]
16. Monterroso-Checa, A.; Teixidó, T.; Gasparini, M.; Peña, J.A.; Rodero, S.; Moreno, J.C.; Morena, J.A. Use of remote sensing, geophysical techniques and archaeological excavations to define the Roman amphitheatre of Torreparedones (Córdoba, Spain). *Remote Sens.* **2019**, *11*, 2937. [CrossRef]
17. Vella, M.A.; Sarris, A. Geophysical survey in archaeological context: A review from Cyprus. *Archaeol. Prospect.* **2022**, *29*, 417–450. [CrossRef]
18. Cella, F.; Fedi, M. High-resolution geophysical 3D imaging for archaeology by magnetic and EM data: The case of the iron age settlement of Torre Galli, Southern Italy. *Surv. Geophys.* **2015**, *36*, 831–850. [CrossRef]
19. Brevik, E.C.; Fenton, T.E.; Lazari, A. Soil electrical conductivity as a function of soil water content and implications for soil mapping. *Precis. Agric.* **2006**, *7*, 393–404. [CrossRef]
20. Al-Gaadi, K.A. Employing electromagnetic induction technique for the assessment of soil compaction. *Am. J. Agric. Biol. Sci.* **2012**, *7*, 425–434.
21. Bourgault, R.R.; Rabenhorst, M.C. Manganiferous Soils in Maryland: Regional Extent and Field-Scale Electromagnetic Induction Survey. *Soil Sci. Soc. Am. J.* **2012**, *76*, 2128–2135. [CrossRef]
22. Schmidt, A. Archaeology, magnetic methods. In *Encyclopedia of Geomagnetism and Paleomagnetism*; Springer: New York, NY, USA, 2007; pp. 23–31.
23. Fedi, M.; Cella, F.; Florio, G.; Manna, M.L.; Paoletti, V. *Geomagnetometry for Archaeology*; Springer: Cham, Switzerland, 2017; pp. 203–230.
24. Lentini, F.; Carbone, S.; Catalano, S. Main structural domains of the central Mediterranean region and their Neogene tectonic evolution. *Boll. Geof. Teor. Appl.* **1994**, *36*, 103–125.
25. Lentini, F.; Carbone, S. Geologia della Sicilia-geology of Sicily. *Mem. Descr. Carta Geologica d'Italia* **2014**, *95*, 7–414.
26. Bernabò Brea, L. Akrai. La Cartotecnica di Scicali e Molino, Catania Italy. 1956. Available online: <https://opac.bncf.firenze.sbn.it/bncf-prod/resource?uri=CUB0094818&v=1&dcnr=0> (accessed on 16 January 2023).
27. Nuzzo, L.; Leucci, G.; Negri, S. GPR, ERT and magnetic investigations inside the Martyrium of St Philip, Hierapolis, Turkey. *Archaeol. Prospect.* **2009**, *16*, 177–192. [CrossRef]
28. Skrame, K.; Di Filippo, M.; Di Nezza, M. Contribution of the Magnetic Horizontal Gradient Operator (MHGO) for the Interpretation of the Magnetic Anomalies. In Proceedings of the Near Surface Geoscience 2016—22nd European Meeting of Environmental and Engineering Geophysics, Barcelona, Spain, 4–8 September 2016; Volume 1, p. 495.
29. Chowanec, R. *Unveiling the Past of an Ancient Town. Akrai-Acrae in South-Eastern Sicily*; Institute of Archaeology, University of Warsaw: Warsaw, Poland, 2015.
30. Lanteri, R. Akrai between Late Antiquity and Byzantine period. In *On the Borders of Syracuse. Multidisciplinary Studies on the Ancient Town of Akrai/Acrae, Sicily*; Chowanec, R., Ed.; Instytut Archeologii: Warsaw, Poland, 2018; pp. 113–122.
31. Leggio, D. Riti e misteri ad Akrai. In *Interpretazione del Complesso Sacro (Scavi 2005–2006)*; Grafica Saturnia: Siracusa, Italy, 2013.
32. Batayneh, A.; Khataibeh, J.; Alrshdan, H.; Tobasi, U.; Al-Jahed, N. The use of microgravity, magnetometry and resistivity surveys for the characterization and preservation of an archaeological site at Umm er-Rasas, Jordan. *Archaeol. Prospect.* **2007**, *14*, 60–70. [CrossRef]

33. Hatakeyama, T.; Kitahara, Y.; Yokoyama, S.; Kameda, S.; Shiraishi, J.; Tokusawa, K.; Mochizuki, N. Magnetic survey of archaeological kiln sites with Overhauser magnetometer: A case study of buried Sue ware kilns in Japan. *J. Archaeol. Sci. Rep.* **2018**, *18*, 568–576. [[CrossRef](#)]
34. Piro, S.; Sambuelli, L.; Godio, A.; Taormina, R. Beyond image analysis in processing archaeomagnetic geophysical data: Case studies of chamber tombs with dromos. *Near Surf. Geophys.* **2007**, *5*, 405–414. [[CrossRef](#)]
35. Godio, A.; Piro, S. Integrated data processing for archeological magnetic surveys. *Lead. Edge* **2015**, *24*, 1138–1144. [[CrossRef](#)]
36. Di Maio, R.; La Manna, M.; Piegari, E. 3D reconstruction of buried structures from magnetic, electromagnetic and ERT data: Example from the archaeological site of Phaistos (Crete, Greece). *Archaeol. Prospect.* **2016**, *23*, 3–13. [[CrossRef](#)]
37. Bigman, D.P. The use of electromagnetic induction in locating graves and mapping cemeteries: An example from Native North America. *Archaeol. Prospect.* **2012**, *19*, 31–39. [[CrossRef](#)]
38. De Smedt, P.; Van Meirvenne, M.; Herremans, D.; De Reu, J.; Saey, T.; Meerschman, E.; Crombè, P.; De Clercq, W. The 3-D reconstruction of medieval wetland reclamation through electromagnetic induction survey. *Sci. Rep.* **2013**, *3*, 1517. [[CrossRef](#)]
39. Won, I.J.; Huang, H. Magnetometers and electro-magnetometers. *Lead. Edge* **2004**, *23*, 448–451. [[CrossRef](#)]
40. Brosten, T.R.; Day-Lewis, F.D.; Schultz, G.M.; Curtis, G.P.; Lane, J.W., Jr. Inversion of multi-frequency electromagnetic induction data for 3D characterization of hydraulic conductivity. *J. Appl. Geophys.* **2011**, *73*, 323–335. [[CrossRef](#)]

Disclaimer/Publisher’s Note: The statements, opinions and data contained in all publications are solely those of the individual author(s) and contributor(s) and not of MDPI and/or the editor(s). MDPI and/or the editor(s) disclaim responsibility for any injury to people or property resulting from any ideas, methods, instructions or products referred to in the content.